AN INTEGRATED APPROACH TO LEVEL-OF-DETAIL BUILDING EXTRACTION AND MODELLING USING AIRBORNE LIDAR AND OPTICAL IMAGERY

F. O. Chikomo*, J. P. Mills, S. L. Barr

School of Civil Engineering and Geosciences, University of Newcastle upon Tyne, Cassie Building, Newcastle upon Tyne, NE1 7RU, UK – (F.O.Chikomo, J.P.Mills, S.L.Barr)@ncl.ac.uk

WG III/4 - Automatic Image Interpretation for City-Modelling

KEY WORDS: Buildings, 3-D, Reconstruction, Level-of-Detail, Laser scanning, Imagery, Integration

ABSTRACT:

The need to automatically extract topographic objects, especially buildings, from digital aerial imagery or laser range data remains an important research priority in both photogrammetric and computer vision communities. This paper describes the proposed model for Level-of-Detail building modelling and progress with the prototype implementation. The paper begins with an overview of the concept of Level-of-Detail, important for adaptive building modelling. Building regions of interest are derived from a normalised digital surface model (nDSM) and regularisation of the roof lines is achieved by a set of contextual constraints with particular emphasis on rectangular buildings. For detailed building reconstruction, the main consideration is given to polyhedral building types with limited support for curvilinear shapes. A moving least squares approach for computation of surface normal vectors and texture metrics is employed for planar segmentation of both gridded data and unstructured point clouds. Delineation of homogeneous planar segments is based on a distance metric between neighbouring local planes. 2-D edge lines derived from the orthoimage are matched with 3-D lines derived from LiDAR based on adjacent plane intersections and then used for the final building reconstruction. Connected regions which fail the local planarity tests and are sufficiently large, are segmented using curvature measures based on least squares quadric surface fitting. Provisional results from the algorithms are promising.

1. INTRODUCTION

1.1 Background

The need to automatically extract 3-D building data from digital aerial imagery or laser range data remains an important research priority in both photogrammetry and computer vision. 3-D building data is important for applications such as city modelling, environmental engineering, disaster mitigation and management and emerging civilian and tactical applications such as virtual and augmented reality and homeland security. Significant success has been achieved so far with semi-automatic building extraction systems using either imagery or LiDAR data, however in restricted domains. The need for an integrated data approach for building extraction has been realised however not yet fully tested. To meet the varying demands in terms of capture of building detail and representation, incorporation of Level-of-Detail (LoD) mechanisms into the building extraction schema has become a necessity. This paper presents an integrated approach for Level of Detail building model reconstruction using airborne LiDAR data and optical imagery and discusses the prototype implementation of the proposed model.

1.2 Related Work

Several algorithms have been proposed for automating the three-dimensional reconstruction of buildings however a robust and versatile solution is yet to be found although significant progress has been made. A discussion of systems based on and accuracies obtainable with photogrammetry and laser scanning in building extraction is contained in Kaartinen et al. (2005). To date, building extraction has largely been based on single data sources, in most cases either LiDAR data alone (Vosselman, 1999; Verma et al., 2006) or images alone (Scholze et al., 2001; Kim and Nevatia, 2004) however the current trend is on integrated data paradigms. Integration of data sets provides multiple cues that can ease the problem of building reconstruction and result in significantly higher levels of automation in the algorithms. The data bases for integrated approaches have included multiple geometric data, GIS layers and bespoke or scene specific knowledge. A number of researchers have demonstrated approaches for combining data for building modelling, for example LiDAR and aerial images (Rottensteiner et al., 2004), LiDAR and three-line-scanner imagery (Nakagawa and Shibasaki, 2003), LiDAR and high resolution satellite images (Sohn and Dowman, 2001), LiDAR and 2-D maps (Overby et al., 2004), aerial images and 2-D maps (Suveg and Vosselman, 2004) and LiDAR, 2-D maps and aerial images (Vosselman, 2002). Schenk and Csatho (2002) discuss theoretical frameworks for multi-sensor data fusion for generic surface description. Not many researchers however have incorporated LoD modelling into their approaches, important for catering for diverse users and applications.

1.3 Level-of-Detail Modelling

The concept of level of detail has been used in computer graphics since the 1970s, mainly for increasing the efficiency of object rendering. Rendering efficiency is achieved by decreasing the visual and geometric detail of 3-D objects as a function of distance from the view point or other metrics such as the perceived object importance. The concept has been adapted and extended for city modelling by the Special Interest Group on 3-D Modelling (Sig3D of the GDI Initiative). LoD building modelling involves adaptable and scaleable extraction and representation of building model information. This enables the capture of building information to be varied depending on the specific requirements of the project and limitations of the building extraction techniques and input data characteristics.

* Corresponding author.

The five levels of detail range from a simple block (2.5-D) model right up to a walkable model, which takes into account both internal and external geometric detail. Figure 1 below illustrates the concept of level of detail modelling as modified for this research. For this research, the aim is to work up to LoD2 with texture effects applied. LoD modelling is important for understanding the trade-offs between model detail and automation potential.

One can possibly identify two main approaches for incorporating the LoD schema into the building reconstruction process. Firstly, a bottom-up approach where a multi-level strategy is adopted for reconstructing each level more or less independently varying the data sets used, their resolution and the algorithmic detail. Secondly, the initial reconstruction effort might be aimed at a detailed level with lower levels derived by building generalisation. A hybrid approach is also possible. In this research, a bottom-up approach is adopted for the multi-level building reconstruction.

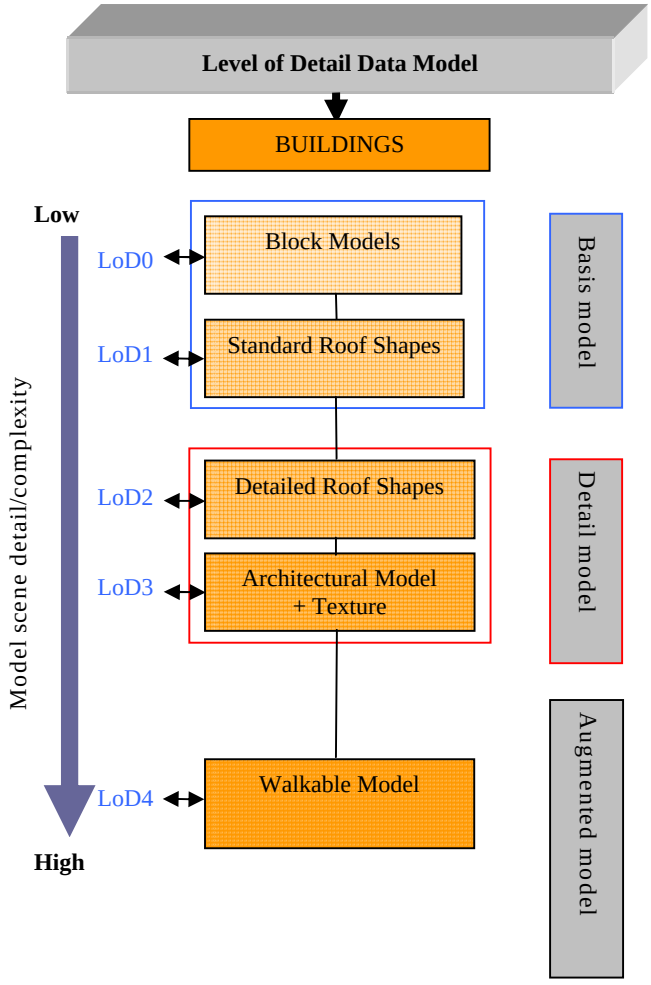

Figure 1. Level-of-Detail modelling schema

1.4 Study Area and Datasets

The study area for the research is Portbury, a small agricultural village, approximately 11 kilometres North West of Bristol, England. Portbury is one of the test sites identified by the Ordnance Survey Research Labs, source of LiDAR data and digital imagery, for research on automated building extraction. The data sets available for the test site are as follows: LiDAR data [16 points/m^2]; digital orthoimagery [GSD 10cm] and OS MasterMap Topography data.

2. ROOFLINE DETECTION

The rooflines are detected from a normalised DSM (nDSM) obtained by differencing an optimised DTM derived from LiDAR using the adaptive TIN algorithm employed in the commercial software TerraScan and an interpolated DSM. A three-metre threshold is applied to the nDSM to detect above ground objects however these include buildings and vegetation. The options followed for vegetation removal included use of intensity data, generic tree point classification, least squares planar fitting differences and near infrared image analysis. The minimum building size was considered to be 12m^2 according to Ordnance Survey specifications. Building segment simplification is achieved using the modified sleeve algorithm and rectangular enforcement is achieved by deriving a moments based orientation and enforcing building line segments to be perpendicular or parallel to this orientation within a defined tolerance. The extracted rooflines define the regions of interest for the geometrical reconstruction of the different levels of detail mentioned before.

3. BUILDING RECONSTRUCTION

3.1 LoD Reconstruction Schema

Reconstruction of LoD0 (block models) requires building rooflines and representative building heights. The building heights are derived from differences of roof and ground heights obtained from a DSM/DTM. LoD1 requires rooflines and LiDAR data for generic roof modelling. LoD2 additionally requires high resolution image data for accurate edge and sub-feature detection and texturing the models.

3.2 Types of Building Surfaces

For this research, consideration is given to two types of surfaces, planar and curvilinear surfaces as shown in Figures 2 and 3 respectively. Planar surfaces are by far the most common type and form the initial hypothesis for the reconstruction algorithms. For curvilinear surfaces, consideration is given to quadric surfaces although this could be extended to more generic superquadric surfaces.

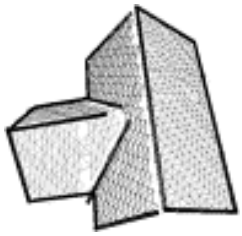

Figure 2. Planar surfaces

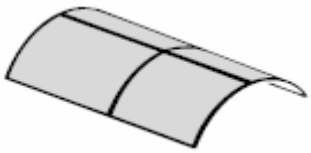

Figure 3. Quadric (curvilinear) surface

3.3 Planar segmentation

For planar segmentation of the LiDAR data, a moving least squares plane fitting algorithm is employed. For each point, a cluster of neighbouring points is determined depending on whether a grid or an unstructured point cloud is used. For gridded data, the algorithm searches for the 8-connected neighbours of each point however the grid resolution can be changed. For unstructured point clouds, the neighbourhood of each point is defined based on either a search radius or a defined number of nearest neighbours within a set maximum distance.

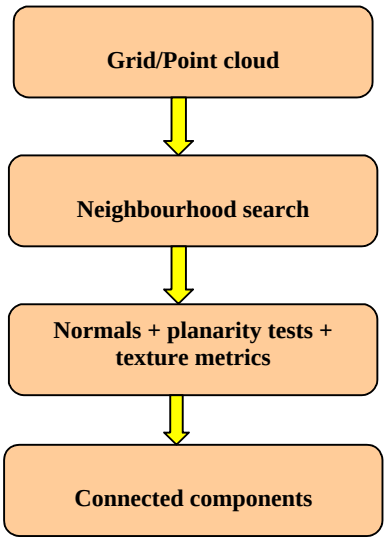

Figure 4. Workflow for planar segmentation

A least squares plane is fitted to the neighbourhood of each point. For each point, a normal vector and texture metrics are computed together with tests for local planarity. Clusters of points lying on the same planes are determined by comparing similarity of normal vector orientations and distances between their local planes. Figure 4 illustrates diagrammatically the steps in the planar segmentation phase of the algorithm. Figure 5 illustrates the vector dispersion and computation of a normal vector for a planar patch. The requirement for this algorithm is to work with both airborne and terrestrial LiDAR data in order to meet the requirements of the different levels of detail.

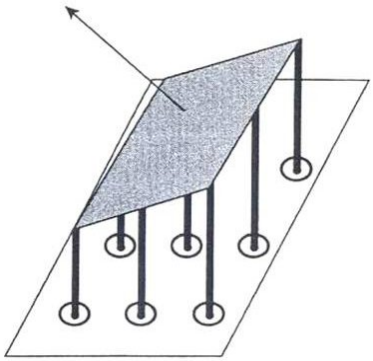

Figure 5. Planar patch normal vector (Parker, 1996)

Applying the planar segmentation to gridded data makes the neighbourhood search easier and allows other image based metrics such as texture coefficients to be calculated however interpolating the point data introduces some unwanted artefacts. Working on scattered point data introduces a computational overhead and requires appropriate adaptation for image based metrics. We experimented with a search radius of 1m.

The planar segmentation algorithm can be summarised as follows:

1. For each data point, locate corresponding points falling within the defined neighbourhood of the point based on the appropriate criteria.
2. For each defined neighbourhood, compute coefficients of the plane and from that compute the normal to the plane for that neighbourhood and the azimuth of the projection of the normal on the *x,y* plane.
3. Compute metrics for assessing local planarity (section 3.5) together with a texture descriptor for each neighbourhood and numerical checks for validating the least squares computation.
4. Data points assumed locally planar are further clustered into consistent planar regions.

3.4 Localised planar fitting of 3-D points

Given a defined neighbourhood $\{(x_i,y_i,z_i)_{i=1,m}\}$ of a point, we want to fit a plane which satisfies the relationship:

$$Z = Ax + By + C \tag{1}$$

where *Z* represents height, *A* and *B* are slope parameters in the *x* and *y* direction respectively and *C* is the offset at the origin.

In the implementation of the algorithms, we consider two forms of minimisation of the residual sums. The first form minimises the sum of residuals in the *z*-direction and the other considers the errors measured orthogonal to the plane and requires use of eigensystem solvers.

3.5 Tests for local planarity

A number of metrics are computed during the point classification phase in order to check if the point is locally planar and weed out erroneous points. The numerical tests are as follows:

- Centre point residual

For each point under consideration, the difference between the actual height value and the height computed using the determined plane parameters should be below a set threshold (Figure 6). In our case, we set the threshold to 0.1 metres based on the average error computed using photogrammetric control points. Equations 2 and 3 mathematically describe the computation of plane coefficients and the centre point residual respectively.

p_1	p_2	p_3
p_4	p_5	p_6
p_7	p_8	p_9

Figure 6. Centre point (p_5) and connected neighbours

$$\left.\begin{aligned} & p_i = (x_i, y_i, z_i) \forall i = 1..9 \\ & E(A,B,C) = \sum_{i=1}^{9} \left[(Ax_i + By_i + C) - Z_i\right]^2 \\ & \nabla E = (0,0,0) \end{aligned}\right\} \tag{2}$$

$$p_5(\text{actual} - \text{calculated}) \le \text{threshold} \tag{3}$$

- Eigen-analysis

The smallest eigenvalue of the dispersion matrix A (Equation 4) computed by reducing neighbourhood points to centre and taking product sums expresses the deviation of the points from the fitted plane. Local planarity is assumed if the smallest eigenvalue is less than a set threshold.

$$A = (P - M)^T (P - M) \quad (4)$$

where *P* is a matrix of neighbourhood points (x_i,y_i,z_i) and M the mean matrix.
A threshold of 0.05 metres was used for the eigen-analysis. This measure of planarity works well for gridded data however a more useful and standardised measure for planarity testing is the ratio of the smallest eigenvalue to the total variance. Fransens (1996) employs a similar method of comparing eigenvalues of the covariance matrix for planarity testing of data in an octree.

- Residual norms

For the residual vectors, the 2-norm (equation 5) is computed and gives a measure of the quality of fit of the model to the data points.

$$\|v\|_2 = (v^T v)^{\frac{1}{2}} \quad (5)$$

3.6 Connected components analysis

The next step is to determine if neighbouring sub-planes defined at each data point could lie on the same planar surface. Our first approach for clustering coplanar points was based on analysing the histograms of normal orientations for each building region of interest and using local peaks for grouping. This approach works well for sloped roofs and fails for flat roofs where the normal vector orientations can shift full circle. A more effective metric for coplanarity considers the distance between neighbouring sub-planes. For each point, the maximum distance between the sub-plane under consideration and surrounding locally planar neighbours. Points with plane distances below a defined threshold are then grouped into consistent clusters. The convex hull of each cluster is then extracted to define boundaries between planes. Final plane parameters for each cluster are determined using the RANSAC algorithm for robustness. The RANSAC algorithm ensures robust fitting of models in the presence of data outliers and requires a large sample of data points. To ensure convergence of the RANSAC algorithm, the inlier threshold is set to 0.05 metres, inlier percentage 75% and the maximum number of iterations 20.

3.7 Planar adjacency and 3-D lines

Planar adjacency graphs are determined for clusters found for each building region of interest. Adjacency is based on the distance between the outer boundaries of the clusters.

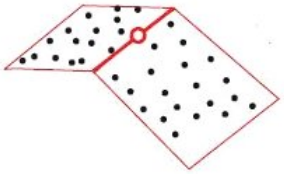

Figure 7. 3-D breakline determination (adapted and modified from Briese, 2004)

Adjacent planes are then intersected to determine 3-D breaklines from LiDAR data, which are then verified and matched against edge lines from the orthoimage. Figure 7 illustrates the basic concept of a 3-D line description derived by intersecting planar patch pairs determined on the basis of clustered point cloud data with the circle representing the support point. The handling of step edges requires further consideration.

3.8 Quadric segmentation

Connected points that are not locally planar and form a sufficiently large size more than $1m^2$ are further tested for curvilinearity. A second degree polynomial surface is fit to the data points and takes the form:

$$Z = a_{20}x^2 + a_{02}y^2 + a_{11}xy + a_{10}x + a_{01}y + a_{00} \quad (6)$$

The steps in the segmentation can similarly be summarised as follows:

1. For each locally non-planar point, define a sufficiently large neighbourhood of points.
2. Use least squares to fit a quadric surface to the local neighbourhood of each point.
3. Compute the derivatives of the surface and the slope of the tangent at each point.
4. Compute curvature measures (Gaussian, Mean and Laplacian) using the derivative and slope of tangent.

A scale factor is applied for numerical optimisation of the computation. Surface modelling is considered additive and applied in a Constructive Solid Geometry fashion. The model could be extended to superquadric surface fitting for more generic curvilinear modelling.

4. IMAGE DATA ANALYSIS

Image data serves to provide more accurate breaklines for detailed modelling, verify 3-D lines derived from LiDAR and allow texture mapping for photorealistic building modelling. There are three important considerations for the integration of high resolution image data:

- Building localisation

Building roofline polygons are localised in the orthoimage by dilating the minimum bounding rectangle then projecting this into the image. A factor of 1.25 is applied to the areal dimensions of the minimum bounding rectangle. This reduces the search space for matching purposes.

- Edge extraction

2-D linear segments are extracted from the orthoimage using the Canny operator implemented in the open source computer vision library, OpenCV.

- Image pruning

The use of high resolution images (GSD 10cm) is required for higher levels of detail. A threshold is applied to remove spurious and short linear segments. To allow matching of the roofline polygons, linear segments parallel to the rooflines, within some tolerance, are retained for shape matching.

5. Provisional results and discussion

This paper outlined a methodology for level of detail building model reconstruction following an integrated data paradigm. A prototype implementation of the proposed model is in progress however most parts of the algorithm have been tested piecemeal. Figure 8 shows an orthoimage of the Portbury test with an area of interest linked to Figures 9 and 10 shown in red.

The test site contains mostly polyhedral buildings. Reconstruction of block models (LoD0) is achieved with minimal effort after processing the DSM/DTM. The planar segmentation algorithm (LoD1+) was applied to interpolated data at four grid resolutions, 1m, 0.5m, 0.25m and 0.10m in order to assess model sensitivity and also applied to the original point clouds.

Figure 8. Orthoimage of the test site (Portbury, Bristol, UK), in red an area of interest linked to Figures 9 and 10

Figures 9 and 10 show colour coded normal vector orientation maps of the small area of interest (in red, Figure 8), derived from the least squares planar fitting algorithm applied over grid DSM data at 25cm and 10cm resolutions respectively. The grid data was derived from point data at 16 points/m^2. 25cm resolution results in a more natural look whereas finer detail is apparent at 10cm resolution. The maps highlight planar surfaces, buildings in particular, very clearly. The reconstruction algorithms are applied to the extracted rooflines. Figure 11 shows an enlarged part of the study site and Figure 12, a colour coded normal vector map in the building regions of interest at 0.50m resolution. The map shows an efficient characterisation of building plane surfaces. The choice of grid resolution needs to be optimised in order to average out noise effects, retain required building geometric detail and optimise the turnaround time.

The planar segmentation algorithm could in principle be applied to terrestrial LiDAR data to meet requirements of LoD3 and above in our modified schema (described in Figure 1).

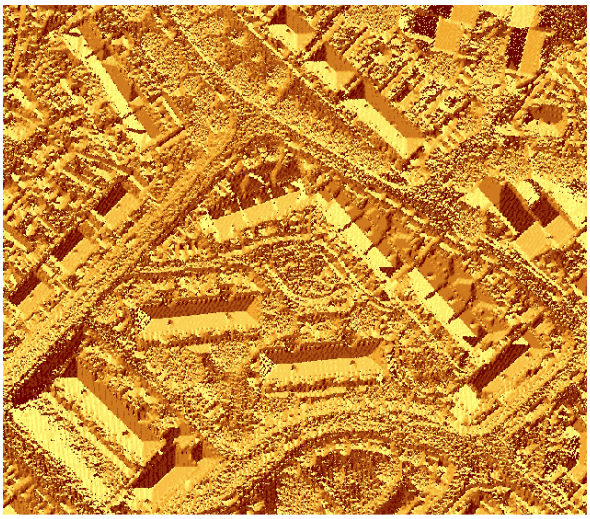

Figure 9. Colour coded normal vector map of the area of interest shown in Figure 8 derived from a gridded LiDAR DSM (25cm resolution) over the area

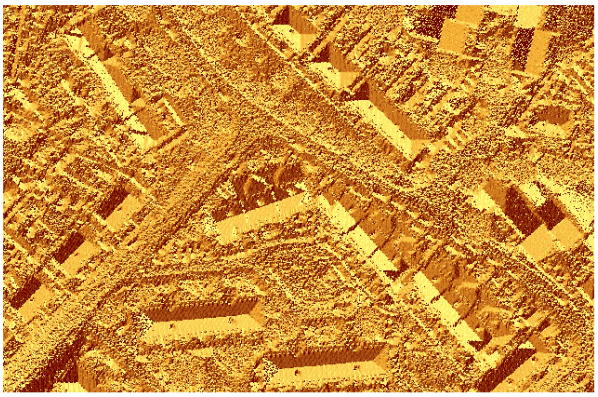

Figure 10. Colour coded normal vector map of the area of interest shown in Figure 8 derived from a gridded LiDAR DSM (10cm resolution) over the area

Figure 11. An enlarged part of the orthoimage for the test site showing building regions of interest linked to Figure 12, different from that shown in Figure 8

Figure 12. Colour coded normal vector map corresponding to image subset in Figure 11

The curvilinear segmentation algorithms have been tested over a different study area with appropriate building types. A significant level of automation in the planar and curvilinear segmentation has been possible. Further work is on labelling connected components and incorporating image edge lines into the segmentation and model reconstruction process. The results are promising.

6. REFERENCES

Baltsavias, E., Greun, A. and Van Gool, L. (2001). Automatic Extraction of Man-Made Objects from Aerial and Space Images. Balkema Publishers, Rotterdam.

Briese, C. (2004). Breakline Modelling from Airborne Laser Scanner Data. Institute of Photogrammetry and Remote Sensing. Vienna, Austria, Vienna University of Technology: 74pp.

Chen, L. C., Teo, T. A., Shao, Y. C., Lai, Y. C., Rau, J. Y (2004). Fusion of LiDAR data and optical imagery for building modelling. ISPRS Commission IV Workgroup 7, Istanbul.

Chikomo, F. O., Mills, J. P., Barr, S. L. (2006). Experimental comparison of LiDAR and image based semi-automatic building extraction systems. Paper presented at ILMF 2006, Denver, Colorado, USA.

Fransens, J. (2006). Statistical segmentation for computer graphics. Expertise Centre for Digital Media. Hasselt, University of Hasselt, Belgium. PhD Thesis: 124pp.

Kaartinen, H., Hyyppä, J., Gülch, E., Hyyppä, H., Matikainen, L., Vosselman, G., Hofmann, A.D., Mäder, U., Persson, Å., Söderman, U., Elmqwist, M. Ruiz, A., Dragoja, M., Flamanc, D., Maillet G., Kersten, T. , Carl, J., Hau, R. , Wild, E., Frederiksen, L., Holmgaard, J. and Vester, K. (2005). EuroSDR building extraction comparison. ISPRS Hannover Workshop 2005 "High-Resolution Earth Imaging for Geospatial Information". May 17-20, 2005, Hannover, Germany.

Kim, Z., Nevatia, R. (2004). Automatic description of complex buildings from multiple images., Computer Vision and Image Understanding 96(1): 60-95.

Nakagawa, M., Shibasaki, R. (2003). Integrating high resolution airborne linear CCD (TLS) imagery and LiDAR data. 2nd GRSS/ISPRS Joint. Berlin, Spring Verlag.

Overby, J., Bobum, L., Kjens, E., Ilsoe, P. M. (2004). Automatic 3D building reconstruction from airborne laser scanning and cadastral data using Hough Transform. ISPRS Commission III: 6pp.

Parker, J. R. (1996). Algorithms for image processing and computer vision. United States of America, John Wiley & Sons, Inc. 417pp.

Peternell, M., Steiner, T. (2004) Reconstruction of piecewise planar objects from point clouds. Computer-Aided Design 36: 333 - 342.

Rottensteiner, F., Trinder, J., Clode, S., Kubik, K., Lovell, B. (2004). Building detection by Dempster-Shafer Fusion of LIDAR Data and Multispectral Aerial Imagery. ICPR'04.

Schenk, T., Csatho, B. (2002). Fusion of LIDAR Data and Aerial Imagery for a More Complete Surface Description. ISPRS Commission III, Symposium 2002: 8pp.

Scholze, S., Moons, T. and Van Gool, L., 2001. A probabilistic approach to roof patch extraction and reconstruction. In: [Baltsavias et al., 2001]

Sohn, G., Dowman, I. (2001). Building extraction using LiDAR DEMs and IKONOS images. ISPRS Commission III, WG III/3: 7pp.

Stamos, I., Allen, P. K. (2000). 3-D Model Construction Using Range and Image Data. Computer Vision and Pattern Recognition 2000: 8 pp.

Suveg, I., Vosselman, G. (2004). Reconstruction of 3D buildings from aerial images and maps. ISPRS Journal of Photogrammetry & RS 58: 202-224.

Verma, V., Kumar, R., Hsu, S. (2006). 3D building detection and modelling from aerial LiDAR data. 2006 IEEE Computer Society Conference Computer Vision and Pattern Recognition 2: 2213 - 2220.

Vosselman, G. (1999). Building Reconstruction Using Planar Faces in Very High Density Height Data. International Archives of Photogrammetry and Remote Sensing 32, part 3/2W5: 87-92.

Vosselman, G. (2002). Fusion of laser scanning data, maps and aerial photographs for building reconstruction. IGARSS'02, Toronto, Canada.

7. ACKNOWLEDGEMENTS

We would like to thank OS Research Labs for providing data sets and steering the direction of this research. We also thank NIIRS10 and GTA Geoinformatik GmbH for their assistance with other aspects of the research.